

Decoupling the effects of plasma current, density, and temperature on DIII-D H-mode energy confinement

D. P. Schissel

General Atomics, P.O. Box 85608, San Diego, USA

Abstract. Experiments that decoupled H-mode plasma current, density and temperature have been performed on the DIII-D tokamak by the application of divertor cryopumping. Deuterium ELMing H-mode steady state discharges were operated in the single null configuration with neutral beam heating. A power law dependence of the ELMing thermal confinement was assumed with the result that the thermal energy confinement depends weakly on density and strongly on plasma current. A local power balance analysis generally found that the ion and electron diffusivity was unchanged with an approximate factor of 2 change in density at constant temperature. In contrast, both the electron and ion diffusivities increased with increasing temperature at constant density. These plasmas were simulated with the Rebut-Lallia-Watkins critical temperature gradient model. Our results indicate that the temperature dependence of the model does not fit the DIII-D data; the model was too optimistic at the highest power. However, the density dependence of the model agrees well with DIII-D data.

1. Introduction

Analysis of DIII-D H-mode discharges has found that increasing the plasma current (I_p) increases the energy confinement as well as the plasma density (n_e); the current and density are tightly coupled. Our intentions in these series of experiments was to first break the tight correlation between H-mode density and current. Second, to use this break in the colinearity to test whether the previous assumptions [1] regarding the lack of dependence of thermal energy confinement (τ_{th}) on n_e was valid. Third, to independently study the effect of n_e and temperature (T_e and T_i) on local energy transport with the intention of elucidating some of the fundamental behavior of cross-field energy transport. Using the DIII-D advanced divertor cryopump to lower the H-mode density it was possible to obtain a factor of two range in n_e at fixed I_p which clearly breaks the previous colinearity. With the colinearity broken it was found that the global H-mode thermal energy confinement time depends weakly on n_e and strongly on I_p [2]. Examining local energy transport in the range $0.2 < \rho < 0.8$ found that the electron and ion diffusivity depended weakly on density and strongly on temperature.

2. Experimental Setup

The DIII-D advanced divertor system consists of an integrated divertor bias electrode, a baffle, and an in-vessel cryopump. The transport experiments controlled the density in an ELMing H-mode by a combination of gas puffing and divertor pumping. The pumping rate was controlled by magnetically adjusting the position of the divertor strike point relative to the pumping aperture. For operational stability simultaneous pumping and gas puffing was not allowed.

The deuterium single-null plasmas were operated at $B_t = 2.0$ T, $\kappa = 1.8$, and with the plasma current between 0.75 MA and 1.5 MA. Approximately the first 100 ms of the H-mode was free of edge localized mode (ELM) activity. The remainder of the H-mode had frequent ELM activity and

all of our results were obtained in this phase. Since our chosen time of analysis was during the ELMing phase, a quasi steady state existed where the time rate of change of the stored energy averaged over several ELM periods was close to zero.

Global confinement analysis has been performed in the usual manner [1–2]. The radial energy transport properties were analyzed using the standard steady state power balance technique via the transport code ONETWO with the assumption of purely diffusive heat transport. ONETWO inputs are the measured profiles of n_e , T_e , T_i , Z_{eff} , and the radiated power, together with the magnetic geometry determined from magnetic probe measurements. The diffusivity is defined by the total radial heat flux available for transport divided by the density times the temperature gradient. Transport properties are calculated only between $0.2 < \rho < 0.8$ since there is a lack of experimental data for $\rho < 0.2$ and the substantial ELM activity for $\rho > 0.8$ creates a large uncertainty in the energy transport.

3. Discussion of Results

The first set of discharges [2] were operated at constant neutral beam power (6 MW) while the density and current were varied independently; a factor of two range was achieved in both parameters. The dataset for this subgroup covers $2.8 < n_e (10^{19} \text{ m}^{-3}) < 5.0$ at 0.75 MA and $3.8 < n_e (10^{19} \text{ m}^{-3}) < 8.2$ at 1.5 MA. Fitting the entire dataset, fixing the power dependence, and assuming that τ_{th} depends only on I_p and n_e resulted in

$$\tau_{\text{th}} = 0.18 I_p^{0.91 \pm 0.08} n_e^{0.18 \pm 0.09} P_L^{-0.5} \quad , \quad (1)$$

with units of seconds, MA, 10^{19} m^{-3} , and MW. The I_p and n_e scaling results from this subgroup are, within the stated uncertainty, consistent with the DIII–D/JET scaling [1] and therefore verify the earlier assumption that τ_{th} depends weakly on n_e . In Eq. (1), setting $P_L^{-0.5}$ accounts for the small range in power [$5.7 < P_L \text{ (MW)} < 6.6$] when combining both plasma currents.

In these discharges it is clear that as n_e was increased T_e and T_i responded by decreasing. This decrease in temperature was enough to keep the stored energy ($W \propto \int n T dV$) approximately constant which is consistent with the observation that τ_{th} is independent of density. Therefore, in these discharges density and temperature are inversely coupled.

To eliminate this coupling a second set of discharges were operated at 1.0 MA where T_e and T_i were kept constant by increasing the neutral beam power (P_{NBI}) at higher density. T_e and T_i profiles were matched (Figure 1) in H–mode discharges with an n_e of $2.9 \times 10^{19} \text{ m}^{-3}$ and P_{NBI} of 3.5 MW, and n_e of $5.4 \times 10^{19} \text{ m}^{-3}$ and P_{NBI} of 8.5 MW. The global analysis finds that the τ_{th} values are consistent with Eq. (1). The local analysis finds that the ion diffusivity remains unchanged within the calculated uncertainties [Figure 2(a)]. The electron diffusivity remains unchanged in the core of the discharge but in a small region around $\rho = 0.75$ decreases with decreasing density. The shape of the neutral beam deposition profile, which is peaked on axis, remains very similar at the two densities.

The antithesis of varying the density at fixed temperature is to vary the temperature at fixed density. A series of discharges were operated with P_{NBI} of 4.7 MW and 13.6 MW at an n_e of $5.0 \times 10^{19} \text{ m}^{-3}$ and I_p of 1.0 MA. Globally τ_{th} of these discharges agrees with Eq. (1). Locally, both the electron and ion diffusivities [Figure 2(b)] increase with increasing temperature. At the half radius, the electron diffusivity increases by approximately $T_e^{3/2}$ and the ion diffusivity by T_i .

4. Simulation of Plasma Energy Transport

Modeling of these discharges employs the simulation capabilities of the ONETWO transport code utilizing the recently modified Rebut–Lallia–Watkins (RLW) critical temperature gradient model for energy transport [3]. The RLW model was modified by changing the ratio of χ_i/χ_e of the standard RLW to give ions a Bohm–like scaling. The H–mode edge transport barrier is simulated using the Hinton–Staebler transport suppression model [4] which assumes that the edge turbulence is suppressed by sheared $\mathbf{E} \times \mathbf{B}$ flow. This edge suppression term acts to reduce the RLW diffusivity. The width and intensity of the Hinton–Staebler suppression is adjusted for each discharge so that

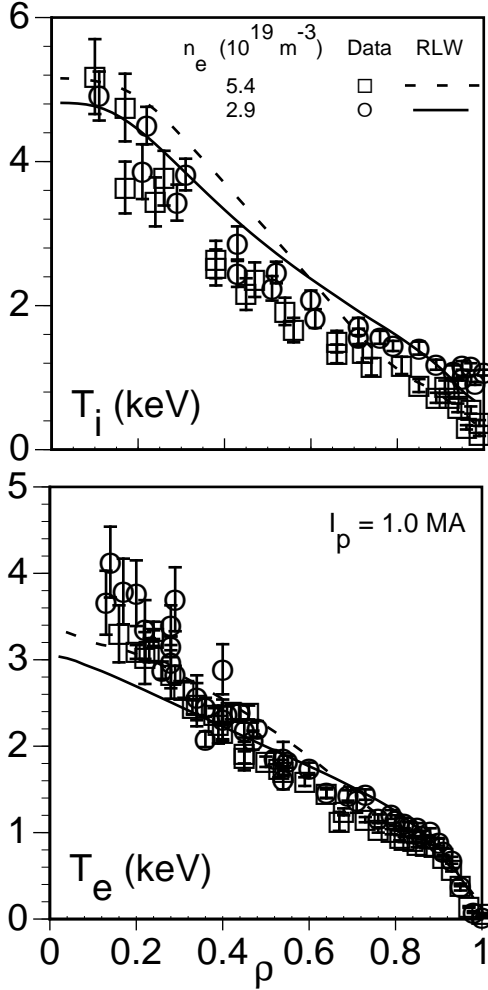


Figure 1. T_i and T_e profiles matched at different densities. RLW simulation fits the data reasonably well.

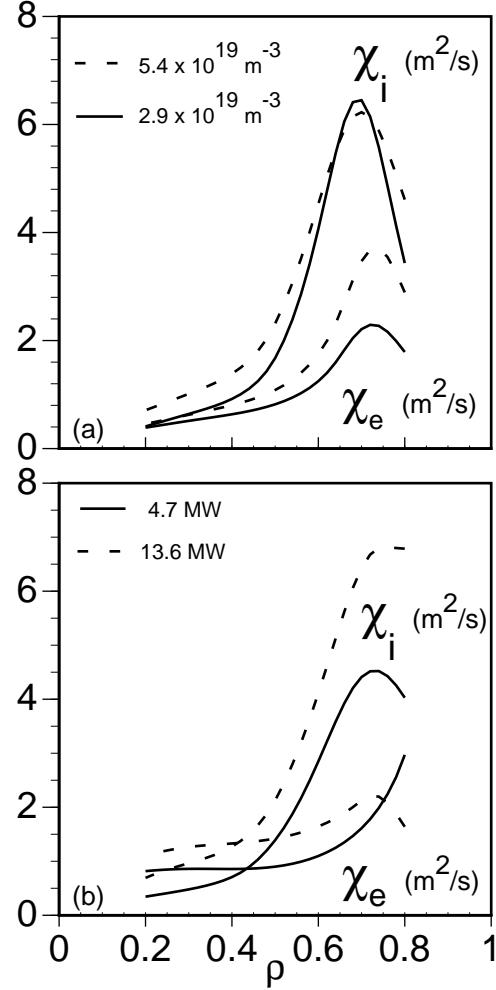


Figure 2. Power balance ion and electron diffusivities (a) remain mostly unchanged in the density scan at 1.0 MA, and (b) increase with temperature in the temperature scan at 1.0 MA and $5.0 \times 10^{19} \text{ m}^{-3}$.

the experimentally measured ($\rho > 0.9$) T_e and T_i gradients are properly modeled. Inside of this edge region ($\rho < 0.9$) the plasma is simulated using the RLW electron and ion diffusivities.

The results of the RLW simulation of the two discharges at constant temperature but different density are shown in Figure. 1. T_e in the higher density discharge is well simulated while the T_i is overestimated in the core of the plasma. Reducing n_e at constant temperature results in a better simulation of T_i and a slight overestimate of the T_e inside of $\rho = 0.3$. These results indicate that the density scaling of the RLW model agrees reasonably well with DIII-D data. The edge of these two discharges was able to be modeled with the same values of the Hinton–Staebler coefficients. The simulation results of the constant n_e different temperature discharges are shown in Figure 3. Both the T_e and T_i profiles are well simulated at low power but are overestimated inside $\rho = 0.5$ at the higher power. For both of these discharges the Hinton/Staebler coefficients needed to be adjusted to properly match the plasma edge.

These discharges have also been compared to the dimensionally correct version of the Hsieh transport model [5] which was developed by studying L- and H-mode plasmas and assuming that the thermal diffusivity has a power law dependence on the temperature gradient scale length. The electron diffusivity is calculated by adding the anomalous term χ_H

$$\chi_H = C_e \left(\frac{n_e T_e^{3/2}}{m_i^{1/2} B_p^2} \right) r \left(\frac{r}{T_e} \frac{\partial T_e}{\partial r} \right)^2, \quad (2)$$

to the ion neoclassical value ($\chi_e = \chi_H + \chi_i^{\text{neo}}$) and the ion diffusivity is calculated by multiplying a constant times the electron diffusivity ($\chi_i = C_i \chi_e$). The comparison was done by determining, in a least squares sense, the electron (C_e) and ion (C_i) multiplier. In the density scan, the ion and electron multipliers were the same within the uncertainties indicating that the Hsieh model adequately describes the change in density. The temperature scan also had similar multipliers between the two discharges. However, comparing the density to the temperature scan finds that the ion multiplier stays the same while the electron multiplier must be reduced by a factor of 2. This result indicates that an additional functional dependence might be required to properly describe the electron transport.

5. Discussion and conclusions

For the first time in the DIII-D H-mode confinement regime, orthogonal I_p - n_e and n_e - T_e scans have been obtained by utilizing the in-vessel divertor cryopump. The insensitivity of energy transport to the density profile justifies previous assumptions made in empirical H-mode scalings that the density scaling of confinement was weak. The ability of the RLW model to simulate energy transport at different densities lends credence to ITER performance predictions. ITER is presently designed near twice the Greenwald limit, an operating density significantly higher than exists in present tokamaks. However, the inability of the RLW model to simulate the higher power DIII-D discharge must be investigated in greater detail.

Acknowledgment

The author acknowledges fruitful discussions with Drs. DeBoo, Mahdavi, Staebler, and St. John. Work supported by the U.S. Department of Energy under Contract No. DE-AC03-89ER51114.

References

- [1] Schissel D.P. *et al.* 1991 *Nucl. Fusion* **31** 73
- [2] Schissel D.P. *et al.* 1994 *Nucl. Fusion* **34** 1401
- [3] Rosenbluth M. *et al.* *Plasma Phys. and Contr. Nucl. Fusion Research*, to be published
- [4] Hinton F.L. and Staebler G.M. 1993 *Phys. Fluids* **B5** 1281
- [5] Hsieh C. *et al.* 1994 *Bul. Am. Phys. Soc.* **39** 1645

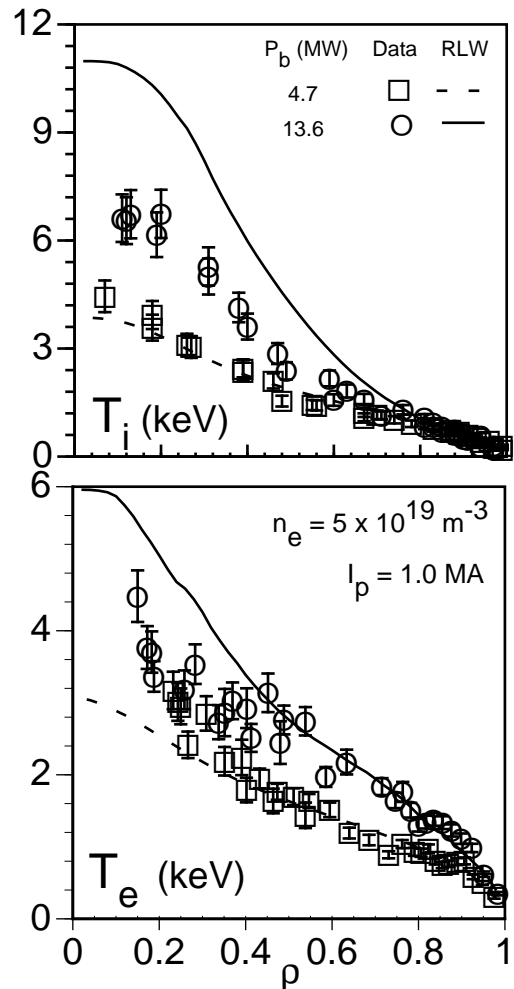


Figure 3. RLW simulation fits the data well at low temperature but is too optimistic at high temperature.